The role of skin layer heat transfer in the surface energy balance

Anne Verhoef [1,3] and Pier Luigi Vidale [2,3]

[1] *Department of Geography and Environmental Science, University of Reading, UK - a.verhoef@reading.ac.uk*

[2] *Department of Meteorology/NCAS-Climate, University of Reading, UK*

[3] *Walker Institute, University of Reading, UK*

Abstract

This paper discusses the seasonal and average diurnal course of the skin layer heat flux, and its determining components, i.e. the temperature gradient and conductivity over the skin layer, Λ_{sk}, which is composed of the vegetation layer, the top layer of the bare soil, or the top layer of the snow pack. Values of G_{sk} are derived from the remainder of net radiation minus the turbulent atmospheric heat fluxes; data used were gathered for CEOP and FLUXNET grass and forest sites.

The course of G_{sk} varies as a function of time of day and time of year (nighttime fluxes have smaller and generally negative values; during the daytime values are positive and are higher when solar elevation increases). Courses and magnitude of G_{sk} for grass and forest sites are comparable. Skin conductivity can take on negative values when the signs of G_{sk} and the temperature gradient do not coincide, as is the case for dense forest, where countergradient heat flux occurs in the vegetation layer. Daytime skin conductivity, Λ_{sk}, is generally larger than the values used by ECMWF and lower during the night. Furthermore, Λ_{sk} appears to depend considerably on atmospheric stability. We conducted some preliminary sensitivity experiments with H-TESSEL, where we adapted Λ_{sk} to more locally suitable values (for grass and forest), either kept at constant levels (with different values depending on whether it was daytime or nighttime) or calculated as a function of the universal profile stability functions (limited to positive values, the model proved unstable for negative values of Λ_{sk}). Multi-year seasonal climatologies of surface temperatures indicated a considerable sensitivity, especially during the nighttime. We recommend further study of the actual model output time series, focusing on the diurnal cycle under different synoptic regimes, as the climatologies mask the sensitivities.

1. Introduction

The surface energy balance in the ECMWF land surface model (H-TESSEL) is given by:

$$R_{n,*} = H + LE + G_{sk} \tag{1}$$

with $R_{n,*}$ the net radiation, G_{sk} the skin layer heat flux, and H and LE the turbulent sensible and latent heat fluxes, respectively. G_{sk} represents a diffusive flux for a skin layer, located between the skin level (with a skin temperature, T_{sk}) and the temperature at the centre of the upper soil layer, T_1 (Figure 1), see also Holtslag and de Bruin, 1988; Duynkerke, 1991; Viterbo and Beljaars; 1995; Steeneveld et al., 2006.

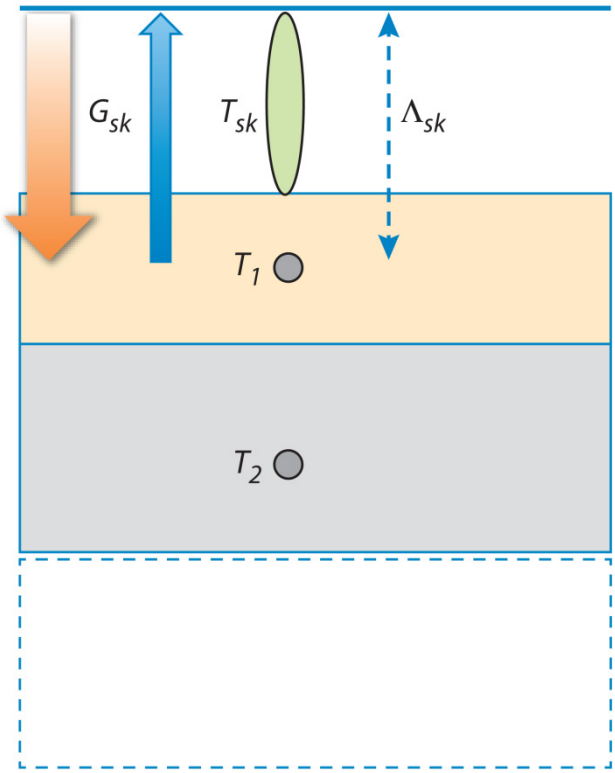

Figure 1. Schematic representation of the skin layer heat flux, G_{sk}, and variables and parameters that play a role in it (see also Eq. 3). T_{sk} is the skin temperature, T_1 is the temperature at the centre of the upper soil layer (T_2 the one of the layer below). Λ_{sk} is the skin layer conductivity.

Net radiation is given by

$$R_{n,*} = (1 - f_{R_s})(R_{s,\downarrow} - R_{s,\uparrow}) + R_{l,\downarrow} - R_{l,\uparrow} \tag{2}$$

where radiation, R, is composed of incoming (downward arrow), outgoing (upward arrow) shortwave (subscript s) and longwave (subscript l) radiative fluxes. This approach takes into account partial absorption of net short-wave radiation, in the skin layer. For low vegetation this factor (f_{R_s}) is 5% of the net shortwave radiation; for high vegetation it is 3%.

Analogously to Fourier's law, G_{sk} is given by

$$G_{sk} = \Lambda_{sk}\left(T_{sk} - T_1\right) \tag{3}$$

The skin conductivity, Λ_{sk}, provides the thermal connection between the skin level (at effective temperature T_{sk}) and the soil or snow deck (see Figure 1), with temperature T_1. The skin represents the vegetation layer, the top layer of the bare soil, or the top layer of the snow pack, has no heat capacity and therefore responds 'instantaneously' to changes in e.g. radiative forcing. T_{sk} can be interpreted as the temperature sensed by an IR thermometer viewing the surface at nadir.

The skin conductivity approach was introduced by Viterbo and Beljaars (1995): a uniform value of 7 W m^{-2} K^{-1} was recommended for all surface types (based on data from the Cabauw grassland site, the Netherlands). Van den Hurk and Beljaars (1996) adapted this approach; they concluded that,

based on measurements collected for a sparsely vegetated vineyard in Spain, a Λ_{sk} value of 7 W m^{-2} K^{-1} should be used for the vegetated part of grid box and 17 W m^{-2} K^{-1} for the bare soil part. The current H-TESSEL employs different values for snow on bare ground/snow on low vegetation (7 W m^{-2} K^{-1}), low vegetation (10 W m^{-2} K^{-1}), bare soil (15 W m^{-2} K^{-1}), and high vegetation, with or without snow (20 W m^{-2} K^{-1} for unstable conditions and 15 W m^{-2} K^{-1}for stable conditions).

This paper studies the diurnal and seasonal variation of G_{sk} and its dependent variables (Λ_{sk} and driving force T_{sk}-T_1) for two surface types (grass and needleleaf forest) using micrometeorological data. It addresses whether the values currently used by ECMWF are adequate and whether Λ_{sk} should really be assumed constant throughout the day.

2. Materials and methods

2.1. Field site descriptions

Table 1 summarises the field sites used in this study; surface types comprised grass and needleleaf forest, in Germany and the Netherlands.

Table 1 Description of the four field sites used in this study.

Location	Falkenberg	Lindenberg	Tharandt	Cabauw
Surface type	Grass	Needleleaf forest	Needleleaf forest	Grass
Latitude	52°10'N	52°18'N	52°58'N	51°97'N
Longitude	14°07'E	13°95'E	13°34'E	4°93'E
Country	Germany	Germany	Germany	Netherlands
Elevation [m a.s.l.]	73	42	380	-1
Topography	Fairly flat	Fairly flat	Gently sloped	Flat
Vegetation height (m)	<0.20	14	26	0.1
LAI (m^2 m^{-2})	<2	5	7.2	<2
Dominant species	Grass	Pine	Norway spruce	Grass
Understorey	n/a	n/a	Wavy hair grass	n.a.
Climate	Marine/continent al (P = 563)	Marine/continental (P = 563)	Mediterranean/ montane (P = 820)	Maritime (P=793)
Reference height (m)	2.4	30.6	42	1.5/5
Length of dataset	2003-2009	2003-2009	1998-2003	2003-2009

2.2. Meteorological variables and fluxes

Radiation-related variables used in this study comprised above-canopy net radiation, R_n, either measured directly with a net radiometer, or calculated from separate values of the four net radiation components presented in Eq. 2. Skin temperature, T_{sk} (°C), was either measured directly with an infrared thermometer or was derived from:

$$T_{sk} = \left[\frac{\left(R_{l\uparrow} - \left(1 - \epsilon_s\right) R_{l\downarrow} \right)}{\left(\epsilon_s \sigma\right)} \right]^{1/4} \tag{4}$$

where ε_s is the surface emissivity and σ the Stefan Boltzmann constant.

Another atmospheric variable used, at reference level, was air temperature, T_a (°C or K).

Eddy covariance data were available for the atmospheric fluxes of sensible heat, H, latent heat, LE, and for friction velocity, u_*.

Soil temperature, T_1, was measured at a depth of approximately 0.05 m. A detailed description of all instrumentation and the experimental set-up for the Falkenberg and Lindenberg site can be found in Beyrich and Adam (2007). For more information on the Tharandt and Cabauw sites see and Grunwald and Bernhofer (2007) and Van Ulden and Wieringa (1996), respectively.

To get a measure of atmospheric stability the universal profile stability functions, Ψ (Paulson, 1970), as a function of $\zeta = (z_r - D)/L$ were calculated, with D the displacement height (taken as $D = {}^{2}/_{3}\, z_{veg}$). Here L is the Monin-Obukhov length given by:

$$L = -\rho C_p u_*^3 \,/\, k \left(\frac{g}{T_a} \right) H \tag{5}$$

where T_a is the absolute air temperature in K, u_* the friction velocity (m s^{-1}), ρ the density of air, k the von Karman constant, g the acceleration of gravity and H the sensible heat flux. For unstable conditions ($\zeta < 0$):

$$\Psi_h = 2.0 \ln\left(\left(1.0 + \left(x^2\right)\right) / 2.0 \right) \tag{6}$$

where

$$x = \left(1.0 - \left(16 - \zeta\right)\right)^{1/4} \tag{7}$$

For stable conditions ($\zeta > 0$) we used

$$\Psi_h = -b\left(\zeta - \frac{c}{d} \right) exp\left(-d\zeta\right) - \left(1 + \frac{2}{3} a\zeta \right)^{1.5} - \frac{bc}{d} + 1 \tag{8}$$

with a=1, b=2/3, c=5, and d=0.35 (largely based on Holtslag and de Bruin, 1988, see IFS, part 4, Eq. 3.22). For neutral conditions $\Psi_h = 0$.

G_{sk} was determined from Eq. 1, i.e. by subtracting H and LE from $R_{n,*}$. We acknowledge that G_{sk} will therefore contain the 'error' resulting from the non-closure of the energy balance, but because we are considering monthly averaged values this effect should be minimal. This issue will be discussed in detail in a follow-up paper. All data required to calculate G_{sk} and related variables, were screened for missing and out of-range values.

3. Results and discussion

3.1. Skin layer heat flux

Figure 2 show the long-term average diurnal course of G_{sk}, per month, for the Falkenberg grass and Lindenberg forest sites. These sites are located within 10 km of each other.

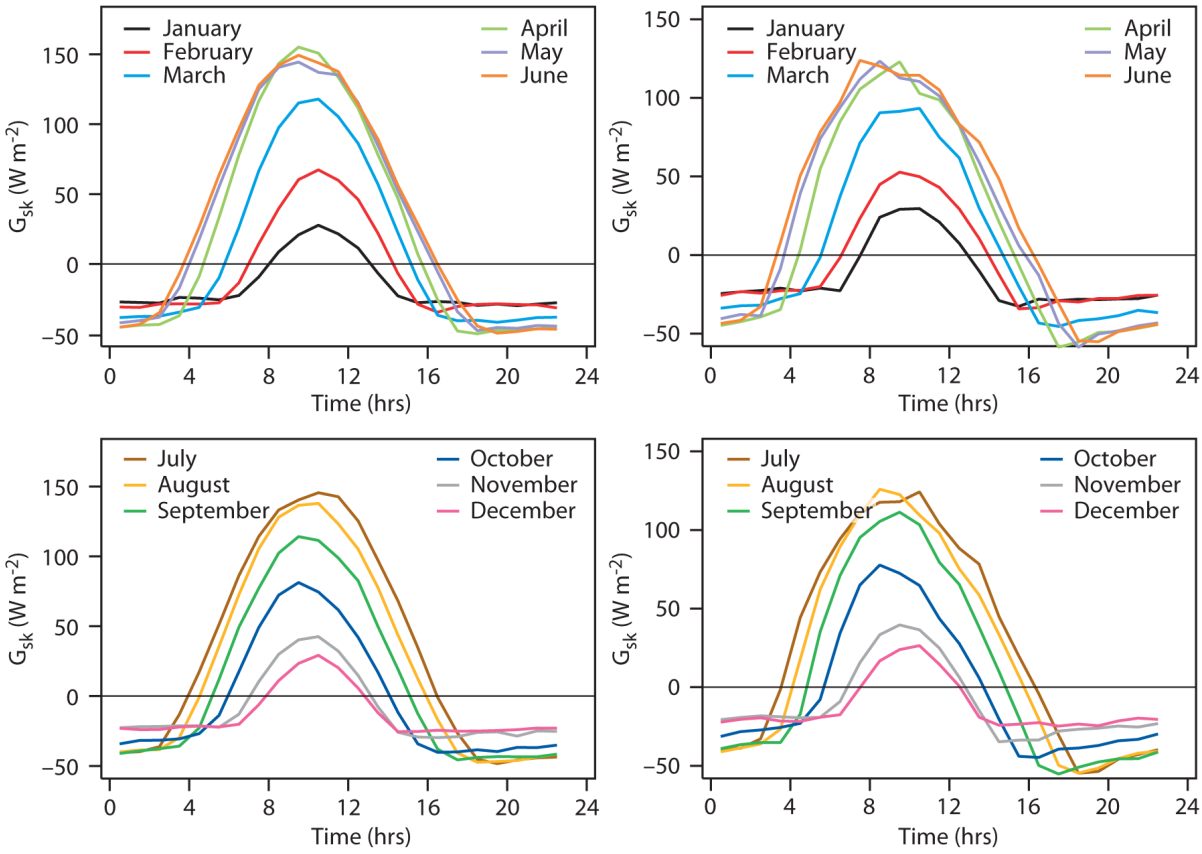

Figure 2. The longterm average diurnal course of G_{sk}, per month, for the Falkenberg grass (left) and Lindenberg forest site (right). The curves have been obtained by averaging the values of G_{sk} obtained for each hour during the day, e.g. between e.g. 1-2 pm, for all days with a certain month. So, with January having 31 days and the dataset consisting of 7 years worth of half-hourly data, each hourly average is based on 31 x 7 x 2 (2 half-hourly values per hour) = 434 datapoints (ignoring missing data).

Figure 2 illustrates that G_{sk} varies diurnally and seasonally. Daytime values ($R_{s,\downarrow} > 0$) are generally positive and nighttime ($R_{s,\downarrow} \sim 0$) values are negative. The amplitudes in G_{sk} increase with day-length, but this is largely a result of an increase in maximum G_{sk}, rather than an increase in minimum G_{sk} (i.e. larger negative values). Therefore, in summer the net daily-integrated G_{sk} takes on relatively large positive values, whereas in the winter months these are slightly negative or ~ 0. Peak G_{sk} values occur between 9-11 am. Positive values for the grass are on average slightly larger than for the forest.

3.2. Difference between T_{sk} and T_1

Fig. 3 shows that, like G_{sk}, the T_{sk}-T_1 gradient also varies diurnally, and its amplitude seasonally. Generally, positive values are representative of daylight conditions and negative values of nighttime conditions, although for some months and surface types values are (on average) always < 0 (January; Cabauw grass) or > 0 (April-August; Tharandt forest) throughout the day. Maximum values for T_{sk}-T_1 are around 7 °C, both for the grass and forest sites, whereas minimum values are ~ -5 °C for the grass site and -1.5 °C for the needleleaf forest.

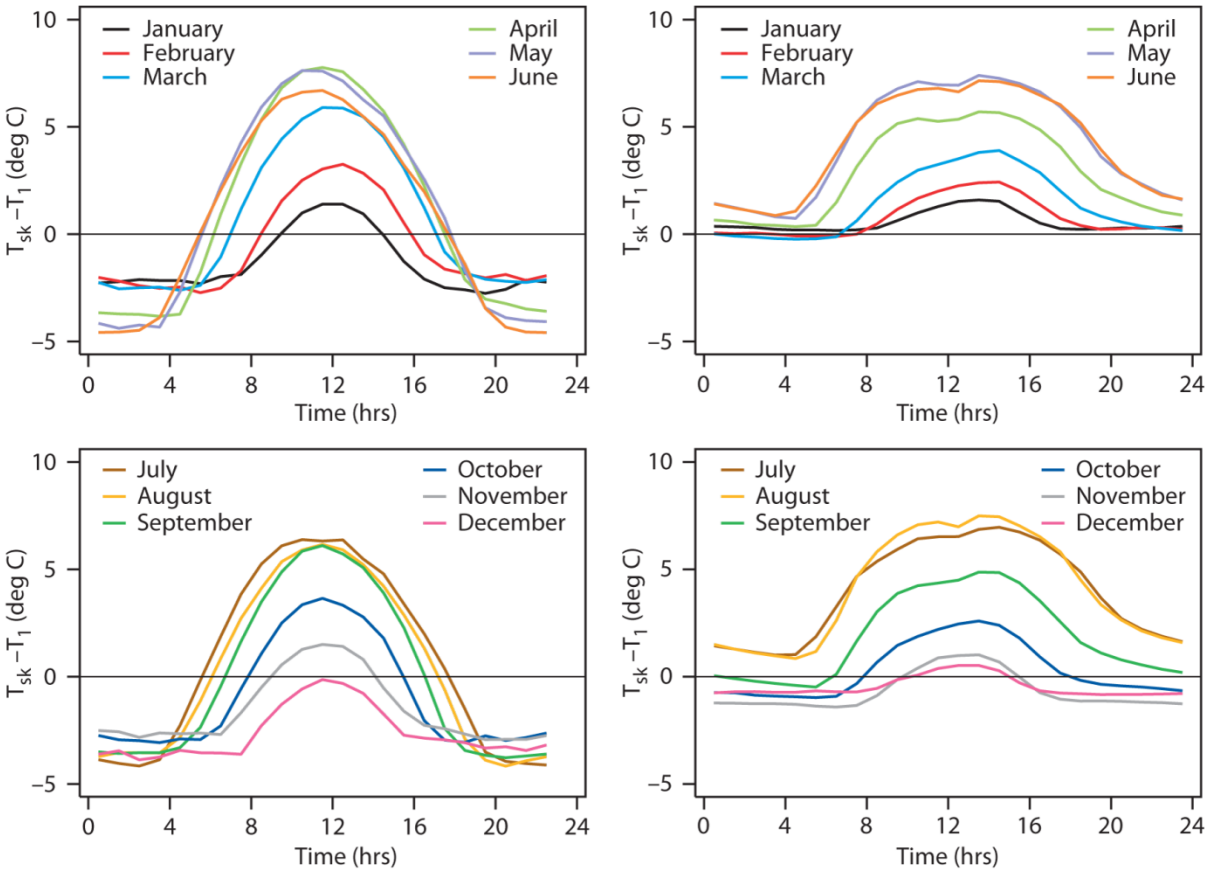

Figure 3. The long-term average diurnal course of T_{sk}-T_1, per month, for Cabauw grass (left) and Tharandt forest site (right). The curves have been obtained by following the procedure described above for Figure 2.

3.3. Skin conductivity

The skin conductivity, presented in Fig. 4, takes on values between -10 and 25 W m^{-2} K^{-1}. Values for Cabauw grassland are only (slightly) negative during morning transition hours (the timing of which varies seasonally), whereas for the Tharandt needleleaf forest Λ_{sk} displays a clear diurnal evolution with strong negative values during the nighttime and positive values during the daytime, for the summer months. During the winter months the diurnal course is less pronounced and at times the nighttime values appear somewhat larger than the daytime values (e.g. October, November, December). For the Falkenberg grass, values ranged between 2-25 W m^{-2} K^{-1} and the peak in Λ_{sk} occurred more towards the noon and was less pronounced (data not shown).

For the Lindenberg forest, Λ_{sk} for the summer months displayed a diurnal course that was more similar to that for Cabauw grass, whereas during the wintermonths it behaved more like Tharandt forest: positive values during the day; negative during the night (data not shown), with values ranging between -10 and 25 W m^{-2} K^{-1}.

Skin conductivity can be viewed as an effective conductivity that is influenced by both soil and vegetation. For completely bare soil, Λ_{sk} can be related to a physical soil thermal conductivity. However, when a (relatively) dense vegetation cover is present, the heat flow into the soil and vegetation layer will also be affected by heat storage and turbulent exchange within the vegetation. The latter is affected by wind speed and stability regime (stable, unstable, neutral), as well as by the strength of the (in)stability.

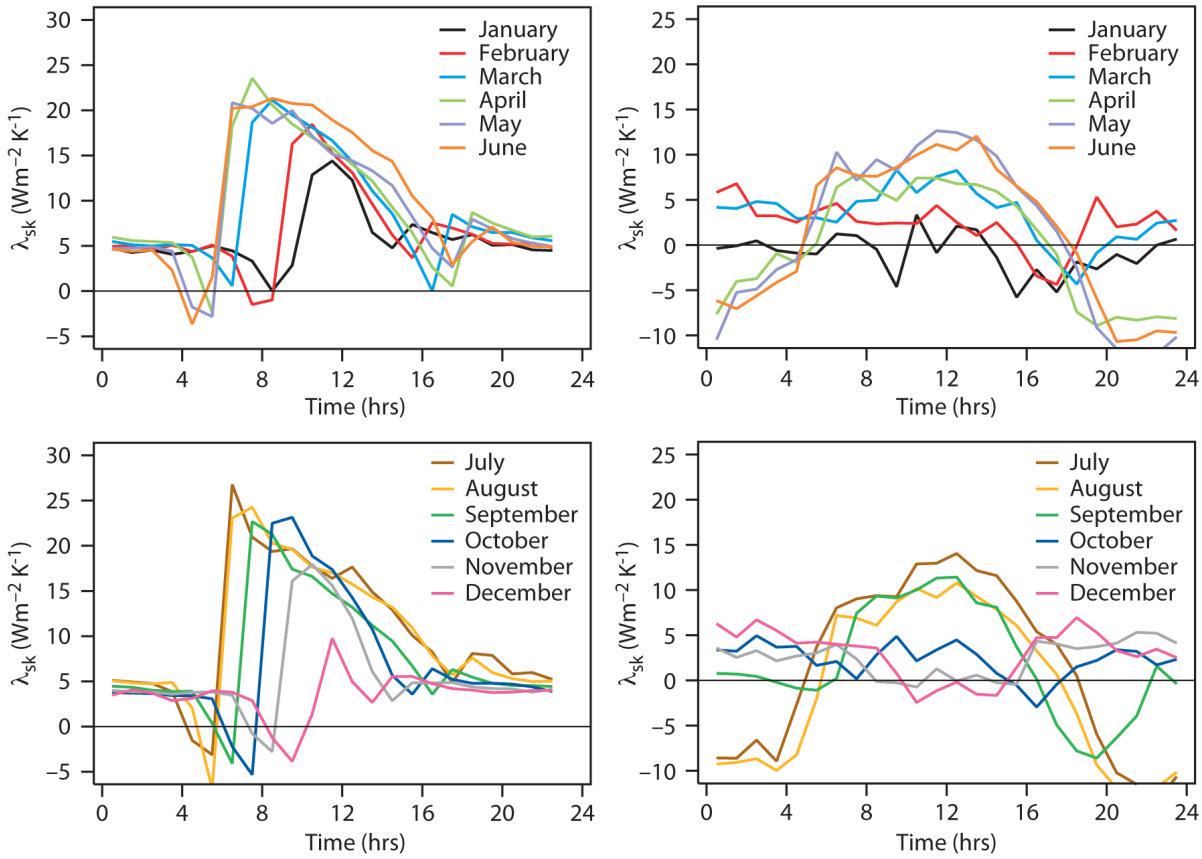

Figure 4. Skin layer conductivity, Λ_{sk}, as calculated from Eq. 3, i.e from $G_{sk}/(T_{sk}-T_1)$, for Cabauw grass (left) and Tharand Forest (right). The median, rather than the average is used here to avoid skewing the values as a result of large Λ_{sk} values when $(T_{sk}-T_1)$~0.

Fig. 5 plots Λ_{sk} as a function of the universal profile stability function, Ψ_h (see Eqs. 6 and 8), for Cabauw grass (left) and Tharand Forest (right). A dependence on stability is evident, with a distinctly different behavior during stable and unstable conditions. The functional dependence of Falkenberg grass Λ_{sk} on Ψ_h was similar to that for Cabauw grass, but under stable conditions, Λ_{sk} increased towards more negative Ψ_h values. The plot of Lindenberg forest looked very similar to the grass, but occasional negative values occurred during the night, although values were never as negative as for Tharandt forest. The reasons for this will be discussed in a follow-up communication.

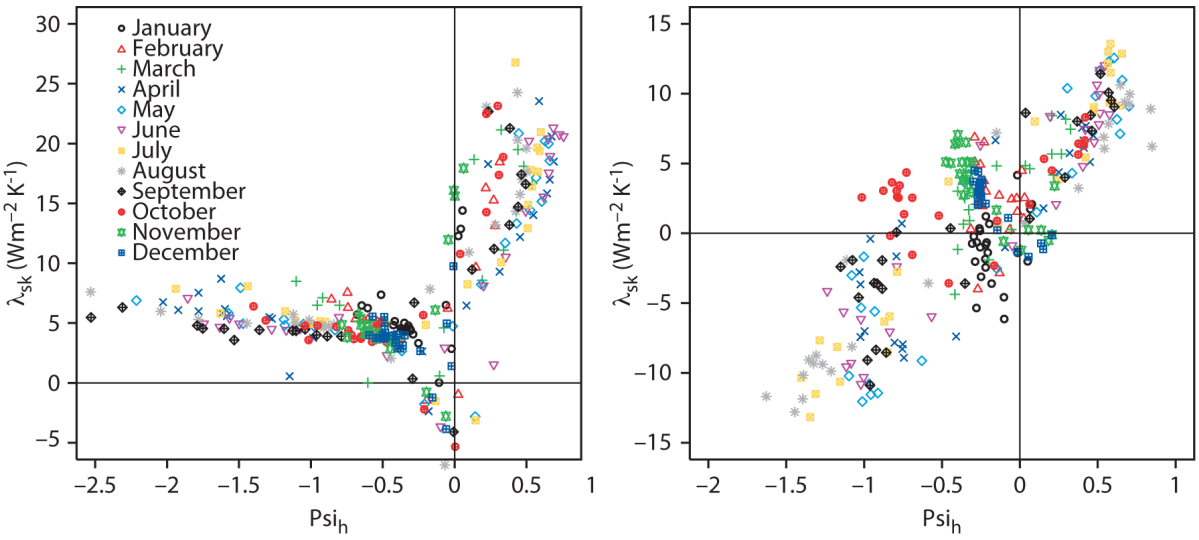

Figure 5. Dependence of skin layer conductivity, Λ_{sk}, as a function of the universal profile stability function, Ψ, for Cabauw grass (left) and Tharand forest (right).

3.4. Preliminary runs with ECMWF H-TESSEL model

As discussed in the Introduction, the current H-TESSEL land surface model developed/used at the ECMWF, which is part of their IFS model (here at cycle 37r3), keeps Λ_{sk} constant on a diurnal (and seasonal) basis for smooth surfaces and surfaces with low vegetation cover. IFS employs Λ_{sk} values of 7 W m^{-2} K^{-1} for snow on bare ground/snow on low vegetation, 10 W m^{-2} K^{-1} for low vegetation, and 15 W m^{-2} K^{-1} for bare soil. Only for high vegetation, with or without snow, it distinguishes between day and night: it uses 20 W m^{-2} K^{-1} for unstable conditions and 15 W m^{-2} K^{-1} for stable conditions. On the basis of Figs. 4 and 5 it is clear that Λ_{sk} is far from constant, both on a diurnal and seasonal basis. It is therefore important to test whether H-TESSEL is sensitive to the choice of Λ_{sk} and whether it is advisable to move away from using a constant prescription of Λ_{sk} and develop a parameterisation for a dynamic Λ_{sk} that depends on surface stability at every time step.

We tested the sensitivity of surface fluxes and prognostics to the specification of different functional forms of Λ_{sk} in H-TESSEL. We distinguish between two broad categories: the first (static) makes use of pre-defined, constant values of Λ_{sk}, one for a thermally stable regime in the surface layer and one for the unstable regime (see Table 2). The second (dynamic) category introduces a new parametrisation of Λ_{sk} based on the surface layer stability, computed by the model at every time step. These different functional forms will be tested for three of the four sites: Cabauw grass, Falkenberg grass and Tharandt forest.

Table 2. Lambda_skin parameters for the two static formulations.

Experiment name	Location	Land cover type	Λ_{sk} stable	Λ_{sk} unstable
CTL	Spatially homogeneous (as in global IFS configuration)	High vegetation	15	20
		Short vegetation	10	10
Constant_Lambda_skin	Spatially homogeneous (adapted for European Experimental sites)	High vegetation	5	20
		Short vegetation	3.3	10

Two static experiments, Control (CTL) and Constant_Lambda_skin, test the impact of different specifications of constant parameters. CTL uses the ECMWF standard values of Λ_{sk}, summarised in Table 2, Constant_Lambda_skin makes use of Λ_{sk} values derived from the observations (third and fourth rows in Table 2), distinguishing between thermal regime (as in CTL for high vegetation) and land cover type (high versus short vegetation).

The dynamic Λ_{sk} experiment (Variable_Lambda_skin) attempted to introduce a dynamic response of Λ_{sk} to the surface layer stability computed by the model, based on Paulson (1970) Ψ stability functions (see Eq. 8). The functional dependence is:

$$\Lambda_{sk} = a\Psi + b \tag{9}$$

Individual curves were derived at each site. Parameters for this dynamic Λ_{sk} formulation, locally adapted for the three European locations, are shown in Table 3. The choice of Λ_{sk} for the stable regime, here limited to positive values, was dictated by the fact that the H-TESSEL model is not yet capable of representing counter-gradient fluxes and thus becomes unstable for negative values of Λ_{sk}.

Table 3. Lambda_skin parameters for the dynamic formulation (eq. 1).

Experiment name	Location	Vegetation type	Stability regime (Ψ)	Λ_{sk} slope, a	Λ_{sk} intercept, b
Variable_Lambda_skin	Cabauw	Short (grass)	stable	-2.5	3.5
			unstable	15	
	Falkenberg	Short (grass)	stable	-2.5	3.5
			unstable	15	
	Tharandt	High (forest)	stable	0	2.5
			unstable	10	

Results were obtained for a matrix of the three experiments at the three sites, for which detailed observations of meteorological drivers and fluxes are available. Fig. 6 shows the sensitivity of the prognostic surface temperature to the three formulations at the three sites (sensible and latent heat fluxes were calculated as well but data are not discussed here). Data are shown for the average diurnal cycle over winter (DJF, top) and summer (JJA, bottom), for six-year climatologies. Nighttime

temperature shows the largest sensitivity (up to 2K colder) when a static dependence on stability with locally representative values (Constant_Lambda_skin) is imposed, in particular over summer at Tharandt forest.

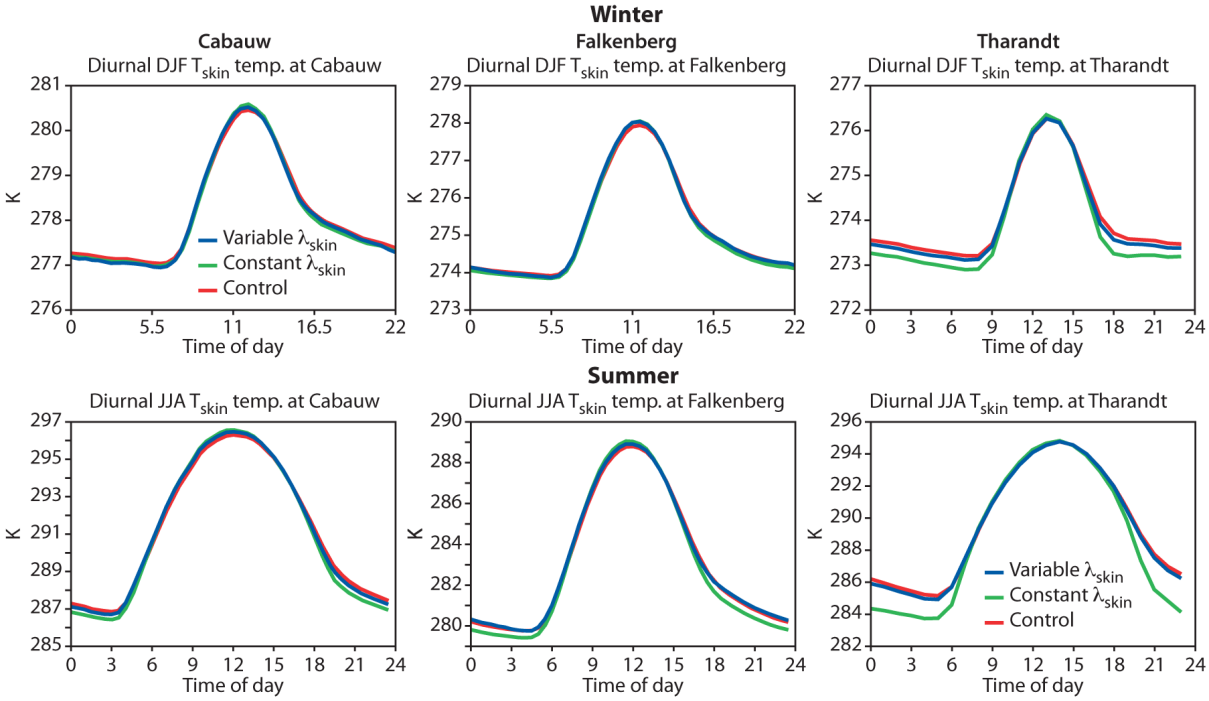

Figure 6. Skin temperature for winter and summer at the three sites: Cabauw (grass), Falkenberg and Tharandt (forest)

Climatologies tend to mask the sensitivity of surface prognostics. Analysis of a portion of the time series shows how, on time scales from diurnal to synoptic, the sensitivity is much larger and again is most prevalent during the nighttime (data not shown).

4. Conclusions

From Sections 3.1-3.4 we can draw conclusions on our observation-based findings. First of all, G_{sk} varies diurnally and seasonally and takes up a large part of net radiation (around 25%, data not shown). Furthermore, Λ_{sk} varies diurnally and seasonally and is a strong function of stability. In some cases Λ_{sk} takes on negative values, possibly as a result of counter-gradient in-canopy transfer, in particular for the taller forest canopies, although it is likely that other effects also play a role (e.g. low level jets or cold air drainage).

For the grass, variation in canopy height may explain part of the scatter in the Λ_{sk} versus stability plots, as well as variation in soil moisture content (via seasonal changes in soil thermal conductivity, data not shown).

The Λ_{sk} values used in the ECMWF IFS model are of the right order of magnitude, but possibly too high for stable conditions and too low for strongly unstable conditions. The increase (in IFS) in Λ_{sk} for high vegetation under unstable conditions (from 15 to 20 W m^{-2} K^{-1}) is warranted, based on the data presented in Figs. 4 and 5. However, these figures seem to suggest that distinguishing between stable and unstable conditions is also advisable for smoother surfaces, such as grass.

Runs with H-TESSEL with Λ_{sk} kept at constant levels (based on the observations presented in this paper) or calculated as a function of the universal profile stability functions (limited to postitive values, the model proved unstable for negative values of Λ_{sk}) indicated a considerable sensitivity for multi-year seasonal climatologies of surface temperatures, especially during the night. We recommend further study of the actual model output timeseries, as the climatologies mask the sensitivities.

Acknowledgements

We thank Frank Beyrich and Fred Bosveld for their help with providing the Lindenberg/ Falkenberg and Cabauw data, respectively. Tharandt FLUXNET files were kindly provided by Reto Stöckli from MeteoSwiss (these data originated from Richard Olson and Eva Falge; Christian Bernhofer is the PI for this site).

References

Beyrich, F. and Adam, W., 2007. Site and Data Report for the Lindenberg Reference Site in CEOP – Phase I. Offenbach a. M. – Selbstverlag des Deutschen Wetterdienstes: *Berichte des Deutschen Wetterdienstes*, 230, ISSN 0072-4130, 55 pp.

Duynkerke, P. G., 1991. Observation of a quasi-periodic oscillation due to gravity waves in shallow radiation fog. *Quart. J. Roy. Meteor. Soc*., **117**, 1207-1224.

Grunwald, T., and Bernhofer, C., 2007. A decade of carbon, water and energy flux measurements of an old spruce forest at the anchor station Tharandt, *Tellus*, Ser. B, **59**, 387–396.

Holtslag, A. A. M., and H. A. R. de Bruin, 1988. Applied modelling of the nighttime surface energy balance over land. *Bound.-Layer Meteor.*, **27**, 689-704.

Paulson, C. A., 1970. The mathematical representation of wind speed and temperature profiles in the unstable atmospheric surface layer. *J. Appl. Meteorol*., **9**, 857-861.

Steeneveld, G.J., van de Wiel, B.J.H. and A.A.M. Holtslag, 2006. Modeling the Evolution of the Atmospheric Boundary Layer Coupled to the Land Surface for Three Contrasting Nights in CASES-99, *J. Atmos. Sci*., **63**, 920-935.

Van den Hurk, B.J.J.M and A.C.M Beljaars, 1996. Impact of Some Simplifying Assumptions in the New ECMWF Surface Scheme. *J. Appl. Meteorol*., **35**, 1333-1343.

Van Ulden A. P. and J. Wieringa, 1996. Atmospheric boundary layer research at Cabauw. *Bound.-Layer Meteor.*, **78**, 39-69.

Viterbo, P. and A. C. M. Beljaars, 1995. An improved land surface parametrization scheme in the ECMWF model and its validation. *ECMWF Tech. Report* No. 75, Research Department, ECMWF.